In Vivo Protection against Retinal Neurodegeneration by Sigma Receptor 1 Ligand (+)-Pentazocine

Sylvia B. Smith,[1,2] *Jennifer Duplantier,*[1] *Ying Dun,*[1] *Barbara Mysona,*[1] *Penny Roon,*[1] *Pamela M. Martin,*[1] *and Vadivel Ganapathy*[3]

Purpose. To evaluate the neuroprotective properties of the sigma receptor 1 (σR1) ligand, (+)-pentazocine in an in vivo model of retinal neurodegeneration.

Methods. Spontaneously diabetic *Ins2*$^{Akita/+}$ and wild-type mice received intraperitoneal injections of (+)-pentazocine for 22 weeks beginning at diabetes onset. Retinal mRNA and protein were analyzed by RT-PCR and Western blot analysis. Retinal histologic sections were measured to determine total retinal thickness, thicknesses of inner–outer nuclear and plexiform layers (INL, ONL, IPL, INL), and the number of cell bodies in the ganglion cell layer (GCL). Immunolabeling experiments were performed using antibodies specific for 4-hydroxynonenal and nitrotyrosine, markers of lipid peroxidation, and reactive nitrogen species, respectively, and an antibody specific for vimentin to view radial Müller fibers.

Results. σR1 mRNA and protein levels in the *Ins2*$^{Akita/+}$ retina were comparable to those in the wild-type, indicating that σR1 is an available target during the disease process. Histologic evaluation of eyes of *Ins2*$^{Akita/+}$ mice showed disruption of retinal architecture. By 17 to 25 weeks after birth, *Ins2*$^{Akita/+}$ mice demonstrated ~30% and 25% decreases in IPL and INL thicknesses, respectively, and a 30% reduction in ganglion cells. In the (+)-pentazocine-treated group, retinas of *Ins2*$^{Akita/+}$ mice showed remarkable preservation of retinal architecture; IPL and INL thicknesses of (+)-pentazocine-treated *Ins2*$^{Akita/+}$ mouse retinas were within normal limits. The number of ganglion cells was 15.6 ± 1.5 versus 10.4 ± 1.2 cells/100 μm retinal length in (+)-pentazocine-treated versus nontreated mutant mice. Levels of nitrotyrosine and 4-hydroxynonenal increased in *Ins2*$^{Akita/+}$ retinas, but were reduced in (+)-pentazocine-treated mice. Retinas of *Ins2*$^{Akita/+}$ mice showed loss of the uniform organization of radial Müller fibers. Retinas of (+)-pentazocine-treated mice maintained the radial organization of glial processes.

Conclusion. Sustained (+)-pentazocine treatment in an in vivo model of retinal degeneration conferred significant neuroprotection, reduced evidence of oxidative stress, and preserved retinal architecture, suggesting that σR1 ligands are promising therapeutic agents for intervention in neurodegenerative diseases of the retina. (*Invest Ophthalmol Vis Sci.* 2008;49:4154–4161) DOI:10.1167/iovs.08-1824

Sigma 1 receptors (σR1) are Ca^{2+}-sensitive, ligand-operated receptor chaperones at the mitochondrion-associated endoplasmic reticulum (ER) membrane.[1] Originally, they were thought to be a subtype of opiate receptor, but it is clear now that σR1 is pharmacologically distinct from other known receptors. Two types of sigma receptors (σR1 and σR2) have been identified[2]; σR1, the better characterized of the two, has been cloned from several species.[3–7] σR1 cDNA predicts a protein of 223 amino acids (M_r 25–28 kDa).[3]

σR1 has been implicated in neuroprotection.[8–14] In the brain, where σR1 is expressed abundantly, ligands for the receptor have been useful in attenuating neuronal loss in in vitro[9,11] and in vivo models of acute neurodegeneration.[10,13,14] Over the past several years, σR1 expression has been analyzed in ocular tissue,[15–21] including the retina.[18–21] RT-PCR analysis amplified σR1 in neural retina and the RPE-choroid complex. In situ hybridization studies revealed abundant expression of σR1 in the ganglion cell layer (GCL), inner nuclear layer (INL), inner segments of photoreceptor cells, and RPE cells.[18] Immunohistochemical analysis confirmed these observations. Recent studies in which primary cultures of mouse Müller cells were used localized σR1 to the ER and nuclear membranes.[21] These cells and other retinal cell types demonstrate robust σR1 binding activity with an apparent K_d of ~25 nM.[21]

The promising evidence of neuroprotection by σR1 ligands in studies of brain tissue coupled with the finding that σR1 is expressed in retina led us to explore the usefulness of ligands for σR1 in retinal degeneration. Our initial studies were performed in vitro using a ganglion cell line, RGC-5,[22] and subsequently using primary ganglion cells isolated from neonatal mouse retina.[8] These studies demonstrated that treatment of cells with (+)-pentazocine, a highly-specific σR1 ligand, led to marked attenuation of cell death induced by the excitotoxins glutamate and homocysteine. These findings suggested that in vivo neurodegenerative diseases of the retina, such as glaucoma and diabetic retinopathy, which result in progressive loss of retinal neurons, may be amenable to treatment with σR1 ligands. Earlier studies, showing that σR1 continues to be expressed in neural retina under hyperglycemic conditions and during diabetic retinopathy,[20] prompted analysis of neuroprotection in this disease.

Diabetic retinopathy, a leading cause of blindness, is characterized by loss of retinal neurons and disruption of vasculature.[23,24] Patients with diabetes lose color and contrast sensitivity within 2 years of onset.[25,26] Focal ERG (electroretinogram) analysis, which detects electrical responses of ganglion cells, reveals dysfunction of these cells early in diabetes.[27,28] Analyses of retinal tissue samples from diabetic patients provide further support of an involvement of retinal neurons in diabetic retinopathy, including detection of several markers of apoptosis.[29] The neuronal death observed in humans has also been reported in rodent models.[30] Using the TUNEL assay, Barber et al.[30] analyzed the retinas of diabetic patients as well as the streptozotocin-induced rat model and

From the Departments of [1]Cellular Biology and Anatomy, [2]Ophthalmology, and [3]Biochemistry and Molecular Biology, Medical College of Georgia, Augusta, Georgia.

Supported by National Institutes of Health, National Eye Institute Grants EY13089 and EY14560.

Submitted for publication February 1, 2008; revised April 14, 2008; accepted July 15, 2008.

Disclosure: **S.B. Smith**, None; **J. Duplantier**, None; **Y. Dun**, None; **B. Mysona**, None; **P. Roon**, None; **P.M. Martin**, None; **V. Ganapathy**, None

The publication costs of this article were defrayed in part by page charge payment. This article must therefore be marked "*advertisement*" in accordance with 18 U.S.C. §1734 solely to indicate this fact.

Corresponding author: Sylvia B. Smith, Medical College of Georgia, Department of Cellular Biology and Anatomy, CB 2820, Augusta, GA 30912-2000; sbsmith@mail.mcg.edu.

Investigative Ophthalmology & Visual Science, September 2008, Vol. 49, No. 9

TABLE 1. Average Mouse Weights and Blood Glucose Levels

Treatment Groups	*n*	Mean Weight ± SEM (g)	Blood Glucose ± SEM (mg/dL)	Age of Mice/Duration of Diabetes (wk)
Pilot Study Testing Two Dosages of (+)-Pentazocine in the STZ-Induced Diabetic Mouse				
Control	4	24.2 ± 1.5	119.5 ± 28.6	14 wk/nondiabetic
STZ-DB	4	19.0 ± 1.8	346.8 ± 21.5	14 wk/10 wk diabetic
STZ-DB/1.0 mg · kg^{-1} (+)-PTZ	2	18.9 ± 1.1	342.0 ± 35.3	14 wk/10 wk diabetic
STZ-DB/0.5 mg · kg^{-1} (+)-PTZ	2	22.5 ± 3.1	471.5 ± 61.5	14 wk/10 wk diabetic
Analysis of σR1 Gene and Protein Expression in the Ins2$^{Akita/+}$ Mouse				
Wild-type	8	21.8 ± 2.2	159.0 ± 39.5	8 wk/nondiabetic
Wild-type (0.5 mg · kg^{-1} (+)-PTZ)	6	23.8 ± 1.3	168.5 ± 33.2	8 wk/nondiabetic
Ins2$^{Akita/+}$	10	21.3 ± 0.9	461.5 ± 57.4	8 wk/4 wk diabetic
Ins2$^{Akita/+}$ (0.5 mg · kg^{-1} (+)-PTZ)	7	22.3 ± 0.9	414.0 ± 35.8	8 wk/4 wk diabetic
Analysis of Effects of 0.5 mg kg^{-1} (+)-PTZ in the Ins2$^{Akita/+}$ Mouse				
Wild-type (no (+)-PTZ)	6	30.2 ± 1.7	104.5 ± 16.3	17–25 wk/nondiabetic
	6	25.2 ± 0.9	153.1 ± 25.3	10 wk/nondiabetic
	4	22.5 ± 1.5	160.5 ± 29.0	7 wk/nondiabetic
Wild-type (0.5 mg · kg^{-1} (+)-PTZ)	9	31.9 ± 0.9	119.8 ± 41.2	25 wk/nondiabetic
Ins2$^{Akita/+}$ (no (+)-PTZ)	9	27.6 ± 2.1	597.3 ± 6.0	17–25 wk/13–21 wk diabetic
	3	23.2 ± 0.4	584.5 ± 21.9	10 wk/6 wk diabetic
	4	21.4 ± 1.1	553.7 ± 44.6	7 wk/3 wk diabetic
Ins2$^{Akita/+}$ (0.5 mg · kg^{-1} (+)-PTZ)	8	25.9 ± 1.6	515.8 ± 44.7	25 wk/21 wk diabetic
Histological Analysis of Fixed Plastic-Embedded Retinal Specimens				
Wild-type	3	27.9 ± 2.5	169.0 ± 22.5	12 wk/nondiabetic
Ins2$^{Akita/+}$	3	27.1 ± 1.2	596.5 ± 11.4	12 wk/8 wk diabetic
Ins2$^{Akita/+}$ (0.5 mg · kg^{-1} (+)-PTZ)	3	24.7 ± 0.8	571.0 ± 16.4	12 wk/8 wk diabetic

(+)-PTZ, (+)-pentazocine.

observed significantly more apoptotic neurons in retinas of diabetic subjects than in those of control subjects. Similar results were observed by Bek[31] and Kerrigan et al.[32]

Recently, two mouse models of diabetic retinopathy were described in which retinal neuronal loss was reported.[33,34] Spontaneously arising diabetes has been reported in the *Ins2$^{Akita/+}$* mouse, which has a point mutation of the Insulin2 gene leading to hyperglycemia and hypoinsulinemia in heterozygous mice by ~4 weeks.[35] In addition to increased retinal vascular permeability and an increase in acellular capillaries, *Ins2$^{Akita/+}$* mice demonstrate ~20% to 25% reduction in the thickness of the inner plexiform layer (IPL), ~16% reduction in the thickness of the INL, and ~25% reduction in the number of cell bodies in the retinal GCL.[33] Cells in the GCL are immunoreactive for active caspase-3 after 4 weeks of hyperglycemia, consistent with cell death by apoptosis. In an induced model of diabetes, mice made diabetic by multiple injections of the pancreatic toxin streptozotocin, but not maintained on insulin, demonstrated 20% to 25% fewer cells in the GCL by 14 weeks after the onset of diabetes.[34] Data obtained using the TUNEL assay and analysis of active caspase-3 suggested that these neurons die by apoptosis. Viability is compromised in these animals, and most animals die by 16 to 20 weeks after onset of diabetes. Given that retinal neurons die over a relatively short period in these two mouse models, they were ideal for assessing neuroprotection by the σR1 ligand (+)-pentazocine. A pilot study to test (+)-pentazocine dosage was conducted in the streptozotocin-induced model and the comprehensive analysis of neuroprotection was performed in the *Ins2$^{Akita/+}$* model.

MATERIALS AND METHODS

Animals

These studies adhered to the ARVO Statement for the Use of Animals in Ophthalmic and Vision Research. For the pilot study to determine an effective (+)-pentazocine dosage, 3-week old C57Bl/6 female mice, purchased from Harlan Sprague-Dawley (Indianapolis, IN), were made diabetic with streptozotocin, according to our published protocol.[34] C57BL/6J *Ins2$^{Akita/+}$* mice were purchased from The Jackson Laboratory (Bar Harbor, ME). *Ins2$^{Akita/+}$* female mice were bred to wild-type male mice in the animal facilities of the Medical College of Georgia, in accordance with institutional policy for appropriate care and use of animals. Genotyping of *Ins2$^{Akita/+}$* mice was performed per the protocol recommended by The Jackson Laboratory. Retinas of male and female mice were examined; however, only those of the males were used in the morphometric retinal analyses, because disease progression in females is slower and less uniform.[35] Diabetes onset was verified by measuring urine glucose with a urine strip test (Clinistix; Fisher Scientific, Pittsburgh, PA) and blood glucose with a blood glucose meter (Prestige Smart System; Home Diagnostics, Inc., Ft. Lauderdale, FL). Fasting blood glucose levels >250 mg/dL were considered diabetic. Diabetic animals were not maintained on insulin. Age-matched, nondiabetic wild-type mice were used as the control. All mice received food and water ad libitum and were maintained on a 12-hour light–dark cycle. Body weight and blood glucose were measured at the time of death (Table 1).

Administration of (+)-Pentazocine

A total of 101 mice were used in these experiments: 12 were used in the pilot study assessing (+)-pentazocine dosage in the streptozotocin-induced diabetic model, and 89 were used to assess (+)-pentazocine in the *Ins2^{Akita}* model. Mice were distributed over four groups: diabetic plus (+)-pentazocine treatment, diabetic with no treatment, nondiabetic plus (+)-pentazocine treatment, and nondiabetic with no treatment (Table 1). At the time of diabetes onset (or comparable age in nondiabetics), the mice were injected intraperitoneally with (+)-pentazocine (Sigma-Aldrich, St. Louis, MO) that had been dissolved initially in DMSO and diluted with 0.01 M PBS. For the streptozotocin-induced diabetic mice, (+)-pentazocine was administered via intraperitoneal injection at two dosages: 0.5 mg · kg^{-1} or 1.0 mg · kg^{-1} three times per

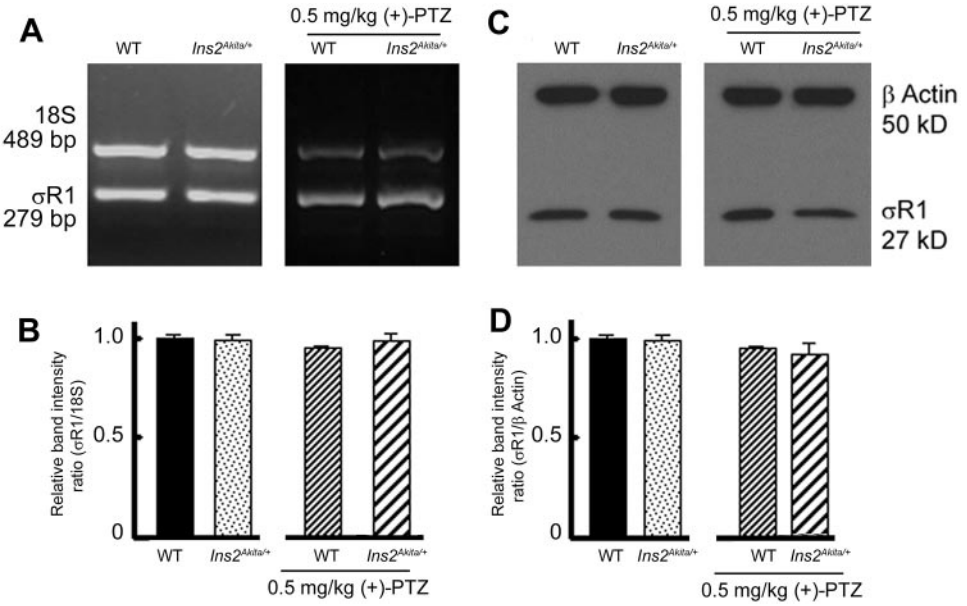

FIGURE 1. σR1 mRNA and protein levels. (**A**) Total RNA was isolated from neural retinas of wild-type and *Ins2*$^{Akita/+}$ mice (age, 8 weeks; 4 weeks diabetic), which had been maintained in the absence or presence of 0.5 mg · kg^{-1} (+)-pentazocine (two times/wk IP; 4 weeks). RNA was subjected to semiquantitative RT-PCR with primer pairs specific for mouse σR1 mRNA (279 bp). 18S RNA (489 bp) was the internal control. RT-PCR products were run on a gel and stained with ethidium bromide. DNA standards (100 bp to 12.2 kbp) were run in parallel. (**B**) Band intensity, quantified by densitometry, of σR1 cDNA relative to 18S cDNA in control and *Ins2*$^{Akita/+}$ retinas. (**C**) Proteins were extracted from retinas of *Ins2*$^{Akita/+}$ mice (age, 8 weeks; 4 weeks diabetic) and age-matched wild-type mice, which had been maintained in the absence or presence of 0.5 mg · kg^{-1} (+)-pentazocine for 4 weeks. Proteins were subjected to SDS-PAGE, followed by immunoblot analysis with an affinity-purified antibody against σR1 (M_r ~ 27 kDa) or β-actin (M_r ~ 50 kDa) (internal loading control). (**D**) Band density, quantified by densitometry, indicated that σR1 protein levels were similar between wild-type and *Ins2*$^{Akita/+}$ mice, and the levels were not altered by a 4-week treatment with (+)-pentazocine. The ratio of the σR1/β-actin bands of the wild-type (+/+) mice was assigned an arbitrary unit of 1.

week for 10 weeks. Based on the outcome of these pilot studies, *Ins2*$^{Akita/+}$ and wild-type mice received intraperitoneal injection of (+)-pentazocine (0.5 mg · kg^{-1}) two times per week for 22 weeks.

RT-PCR and Immunoblot Analysis to Detect σR1

The neural retina was dissected from the remainder of the eye cup of *Ins2*$^{Akita/+}$and wild-type mice. Three to four eyes per group per experiment were pooled for analysis. For gene expression, total RNA was isolated (TRIzol reagent; Invitrogen, Carlsbad, CA). RT-PCR was performed with primer pairs specific for mouse σR1[6]: 5′-CTC GCT GTC TGA GTA CGT G-3′ (sense) and 5′-AAG AAA GTG TCG GCT GCT AGT GCA A-3′ (antisense) (nucleotide position 315-333 and 572-593; expected PCR product size, 279 bp). 18S RNA was the internal standard. RT-PCR was performed at 35 cycles, with a denaturing phase of 1 minute at 94°C, an annealing phase of 1 minute at 59°C, and an extension of 2 minutes at 72°C. A 20-μL portion of the PCR products were gel electrophoresed and stained with ethidium bromide. For protein identification, we performed immunoblot analysis to detect σR1 protein in neural retinas according to our published method.[8] Protein samples were subjected to SDS-PAGE and transferred to nitrocellulose membranes, which were incubated with anti-σR1 antibody (1:500) followed by incubation with HRP-conjugated goat anti-rabbit IgG antibody (1:3000). The proteins were visualized by using a chemiluminescence Western blot detection system. The membranes were reprobed with mouse monoclonal anti-β-actin antibody (1:5000) as a loading control. The films were analyzed densitometrically, as described.[8]

Tissue Processing and Morphometric Analysis

The mice were killed by CO_2 asphyxiation followed by cervical dislocation. The eyes were removed immediately and oriented in OCT (Tissue-Tek; Miles Laboratories, Elkhart, IN), such that the plane of section included the temporal and nasal ora serrata. Left and right eyes were frozen slowly by immersion in liquid nitrogen (without fixation); 10-μm-thick cryosections were prepared as described.[36] Cryosections were stained with hematoxylin and eosin (H&E) and used for systematic morphometric analysis with a fluorescence microscope (Axioplan2 equipped with HRM camera and the Axiovision 4.6.3 program; Carl Zeiss Meditec, Dublin, CA). Measurements included the thickness of the total retina, IPL, INL, outer plexiform layer (OPL), and the photoreceptor inner/outer segments. The number of rows of photoreceptor cell nuclei in the outer nuclear layer (ONL) was counted. The number of cell bodies in the GCL was quantified by counting cells from the temporal ora serrata to the nasal ora serrata and expressing the data as number of cells per 100-μm length of retina. Sections analyzed were from the center of the eyeball, thus the optic nerve was visible. Three measurements were made on each side (temporal and nasal) of the optic nerve at 200- to 300-μm intervals resulting in six measurements obtained per eye. Both eyes were analyzed in each mouse. In addition, the eyes of nine mice (three wild-type, three *Ins2*$^{Akita/+}$, and three (+)-pentazocine-treated *Ins2*$^{Akita/+}$, age: 12 weeks) were enucleated and fixed for 1 hour at room temperature in 2% paraformaldehyde and 2% glutaraldehyde in 0.1 M cacodylate buffer in sucrose and postfixed for 1 hour with osmium tetroxide. Processing and embedding of tissue in resin (EMbed-812; Electron Microscopy Sciences, Hatfield, PA) was performed according to our published protocol.[37]

TUNEL Assay and Immunodetection of Vimentin, 4-Hydroxynonenal, and Nitrotyrosine

Retinal cryosections were subjected to a TUNEL assay (ApopTAG Fluorescein *In Situ* Apoptosis Detection Kit; Chemicon, Temecula, CA), according to the manufacturer's protocol. They were counterstained with DAPI dye, to label all nuclei. For immunohistochemical detection of vimentin, 4-hydroxynonenal, and nitrotyrosine, retinal cryosections were fixed for 10 minutes in 4% paraformaldehyde prepared in PBS, washed thrice in PBS for 5 minutes, and blocked for 1 hour (PowerBlock; Biogenx, San Ramon, CA). All procedures were performed at 4°C. Sections were incubated in a humidified chamber overnight at 4°C with either mouse anti-human vimentin monoclonal antibody (1:25; Chemicon), rabbit polyclonal anti-4-hydroxy-2-nonenal antibody (1:3000; Alpha Diagnostic, San Antonio, TX) or rabbit anti-nitrotyrosine polyclonal antibody (1:250; Chemicon). In control experiments, some sections were incubated with normal donkey serum instead of the primary antibody. For detection of the primary antibodies, the sections were washed three times in PBS for 5 minutes and incubated with either Oregon Green Alexa Fluor 488–conjugated goat anti-mouse IgG (1:1000) to detect vimentin, or Alexa Fluor 555–

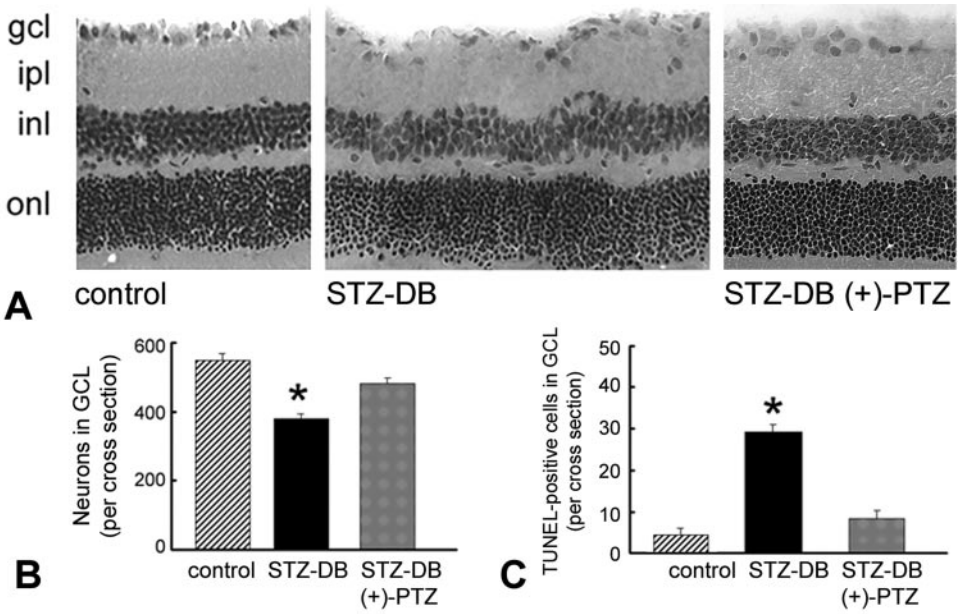

FIGURE 2. Effects of (+)-pentazocine on retinas of STZ-induced diabetic mice. (**A**) Photomicrographs of H&E-stained retinas of control (C57BL/6) mice, STZ-induced diabetic mice that had been diabetic 10 weeks, or STZ-induced diabetic mice treated with 0.5 mg · kg^{-1} (+)-pentazocine over the 10-week period. Note the well-organized morphology of the control and the (+)-pentazocine-treated retinas with dense distribution of ganglion cells compared to the untreated diabetic retina showing fewer cell bodies in the GCL. ipl, inner plexiform layer; inl, inner nuclear layer; onl, outer nuclear layer. (**B**) Number of cell bodies in the GCL of retinal cross-sections from control (nondiabetic) mice, untreated diabetic mice (UN), and diabetic mice treated with 0.5 mg · kg^{-1} (+)-pentazocine (PTZ). (**C**) Number of TUNEL-positive cells in the GCL. *Significantly different from control and PTZ-treated diabetic mice ($P < 0.01$). Error bars, SE.

conjugated donkey anti-rabbit IgG (1:1000) to detect 4-hydroxynonenal and nitrotyrosine (Invitrogen, Carlsbad, CA). Tissues were viewed by epifluorescence with the fluorescence microscope equipped as described earlier and with filters to detect FITC and DAPI. TUNEL-positive (green fluorescing) cells in the GCL, INL, and ONL were counted along the full length of the retina from the nasal to the

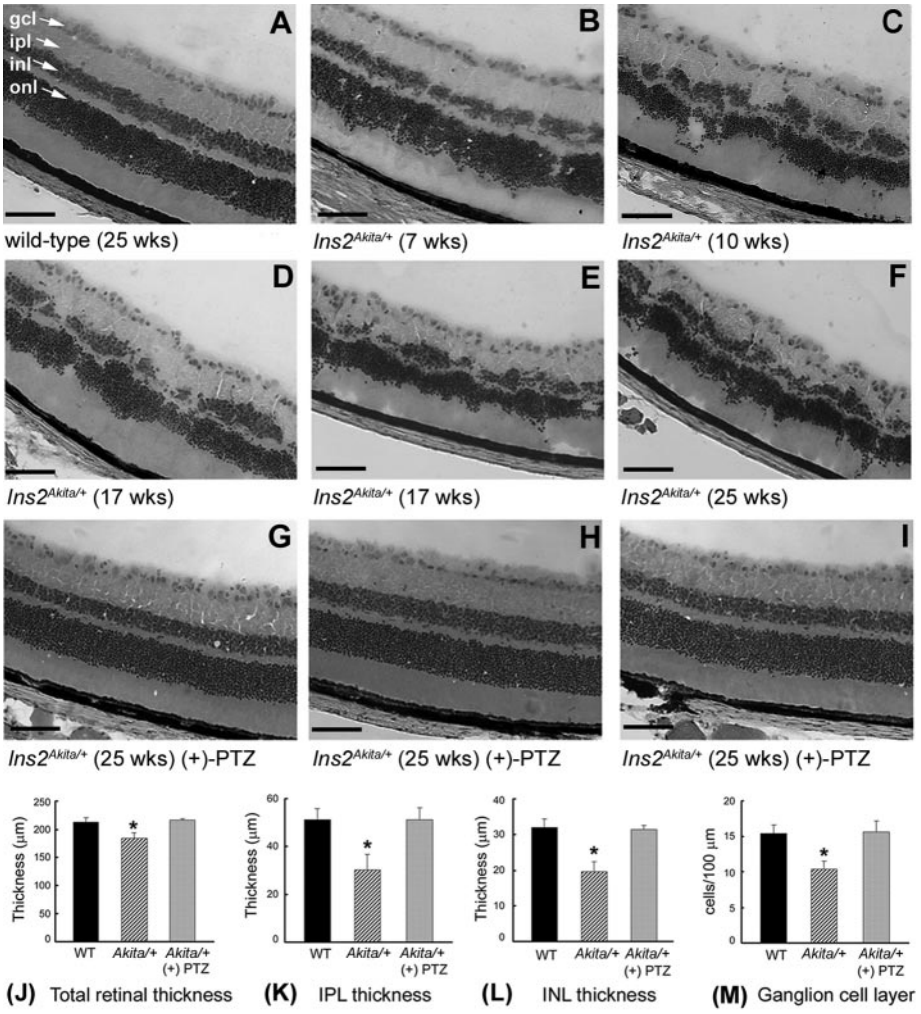

FIGURE 3. Preservation of retinal structure in *Ins2*$^{Akita/+}$ mice administered (+)-pentazocine. Representative H&E-stained retinal cryosections of (**A**) wild-type mice: GCL cells were distributed evenly, and nuclear layers were uniformly thick. (**B–F**) *Ins2*$^{Akita/+}$ mice: INL became disrupted with age, and GCL density decreased. (**G–I**) *Ins2*$^{Akita/+}$mice treated with (+)-pentazocine (0.5 mg/kg, two times/wk IP; 22 weeks) showed marked preservation of retinal layers. PTZ, pentazocine; gcl, ganglion cell layer; ipl, inner plexiform layer; inl, inner nuclear layer; onl, outer nuclear layer. Retinal sections were subjected to morphometric analysis: (**J**) total retinal thickness, (**K**) IPL thickness, (**L**) INL thickness, and (**M**) number of cell bodies in GCL per 100-μm length of retina. Data are the mean ± SE of measurements from retinas of six wild-type (12 eyes), nine *Ins2*$^{Akita/+}$ (18 eyes), and eight *Ins2*$^{Akita/+}$ treated with (+)-pentazocine (16 eyes). *Significantly different from wild-type and (+)-pentazocine-treated mice ($P < 0.001$). Scale bar, 50 μm.

temporal ora serrata. In each experimental group, retinas of five mice were analyzed.

Statistical Analysis

Analysis of variance was used to determine whether there were significant differences in morphologic measurements and in the number of TUNEL-positive cells in diabetic versus nondiabetic, age-matched control mice, as well as in diabetic or age-matched, nondiabetic mice with no treatment versus diabetic mice treated with (+)-pentazocine. The Tukey paired comparison test was the post hoc statistical test. Data were analyzed with commercial software (SPSS, ver. 14; SPSS, Chicago, IL). $P < 0.05$ was considered significant.

Results

σR1 Gene and Protein Expression in Retinas of *Ins2*$^{Akita/+}$ Mice

Before testing neuroprotective effects of (+)-pentazocine, σR1 mRNA and protein expression were analyzed in *Ins2*$^{Akita/+}$ mouse retinas (Fig. 1). The expression levels were comparable to wild-type, suggesting that σR1 is an available therapeutic target in the diabetic retina. These findings were similar to our previously published data showing that σR1 is expressed in neural retina of the streptozotocin-induced diabetic mouse retina.[20]

Effects of Pentazocine on Neuronal Death in Diabetic Retinopathy

The dosage of (+)-pentazocine used in the study with *Ins2*$^{Akita/+}$ was selected based on data from the pilot study of streptozotocin-induced diabetic mice. Histologic sections of retinas from streptozotocin-induced diabetic mice are shown in comparison to control and (+)-pentazocine-treated mice (Fig. 2). The diabetic mice had fewer cells in the GCL, but the retinal architecture was similar to that of the control. Streptozotocin-induced diabetic mice were administered various dosages of (+)-pentazocine (Table 1). At the 0.5-mg · kg^{-1} dosage, (+)-pentazocine reduced cell loss in the GCL (Fig. 2B) and reduced apoptotic neuron death (Fig. 2C). Thus, this dosage was used in the comprehensive analysis of the effects of (+)-pentazocine on retinopathy in the *Ins2*$^{Akita/+}$ mice.

Ins2$^{Akita/+}$ mice were injected intraperitoneally at diabetes onset (~4-weeks of age) with 0.5 mg · kg^{-1} (+)-pentazocine twice weekly for 22 weeks. The progression of changes in *Ins2*$^{Akita/+}$ retinas compared with wild-type over this time period is shown in Figure 3. Wild-type mice had uniform thickness of layers throughout the central and midperipheral retina (Fig. 3A). *Ins2*$^{Akita/+}$ mice had modest INL thinning at 7 weeks (Fig. 3B) and more dramatic INL cell dropout at 10 weeks (Fig. 3C). By 17 to 25 weeks, there was marked INL and GCL cell loss in *Ins2*$^{Akita/+}$ mice (Figs. 3D–F). The IPL, which is composed of synaptic processes of cells in the INL and GCL, was also thinner. The cell loss and misalignment of inner retinal layers resulted in a somewhat wavy appearance in some of the retinas of 17- to 25-week-old *Ins2*$^{Akita/+}$ mice. We found that (+)-pentazocine treatment of *Ins2*$^{Akita/+}$ mice led to marked preservation of retinal architecture. The data shown (Figs. 3G–I) are from retinas of three different (+)-pentazocine-treated *Ins2*$^{Akita/+}$ mice, representative of the excellent retinal structure observed in the eyes of all diabetic mice treated with (+)-pentazocine ($n = 8$ mice, 16 eyes). Morphometric analysis indicated a significant decrease in the thickness of *Ins2*$^{Akita/+}$ mouse retinas, whereas (+)-pentazocine-treated *Ins2*$^{Akita/+}$ mice were comparable to wild-type mice (Fig. 3J). The IPL and INL in *Ins2*$^{Akita/+}$ mice measured 30.3 ± 6.4 and 19.68 ± 2.72 μm, respectively. In (+)-pentazocine-treated *Ins2*$^{Akita/+}$ mice, the values for the thicknesses of the IPL and INL (51.2 ± 4.9 and 31.3 ± 1.3 μm, respectively) were comparable to those in wild-type mice (51.1 ± 4.6 and 31.9 ± 2.4 μm, respectively; Figs. 3K, 3L). There were 30% fewer cell bodies in the GCL of *Ins2*$^{Akita/+}$ mice compared with wild-type mice (10.4 ± 1.2 vs. 15.4 ± 1.2 cells/100 μm retinal length, respectively) whereas the values for (+)-pentazocine-treated *Ins2*$^{Akita/+}$ mice (15.6 ± 1.5 cells/100 μm) were similar to those in wild-type (Fig. 3M). Of note, (+)-pentazocine-treated *Ins2*$^{Akita/+}$ mice remained hyperglycemic throughout treatment. Blood glucose levels were ~500 mg/dL (similar to untreated *Ins2*$^{Akita/+}$ mice) and were significantly higher than those in wild-type mice (104–160 mg/dL; Table 1), suggesting that hyperglycemia per se may not be sufficient to trigger neuronal loss in diabetes.

Assessment of Neuronal Apoptosis and Cellular Stress

Neuronal apoptosis has been reported in *Ins2*$^{Akita/+}$ mouse retinas.[33] We determined the number of TUNEL-positive cells in retinas of (+)-pentazocine-treated versus untreated *Ins2*$^{Akita/+}$ mice (Figs. 4A–C). There were significantly more TUNEL-positive cells in the GCL and INL in retinas of untreated mice than in those of treated and wild-type mice (Figs. 4D, 4E), demonstrating robust neuroprotective effects of (+)-pentazocine in vivo. To assess the effects of diabetes on Müller cells, we visualized the radial fibers by immunolabeling of the intermediate filament protein vimentin, a glial cell marker.

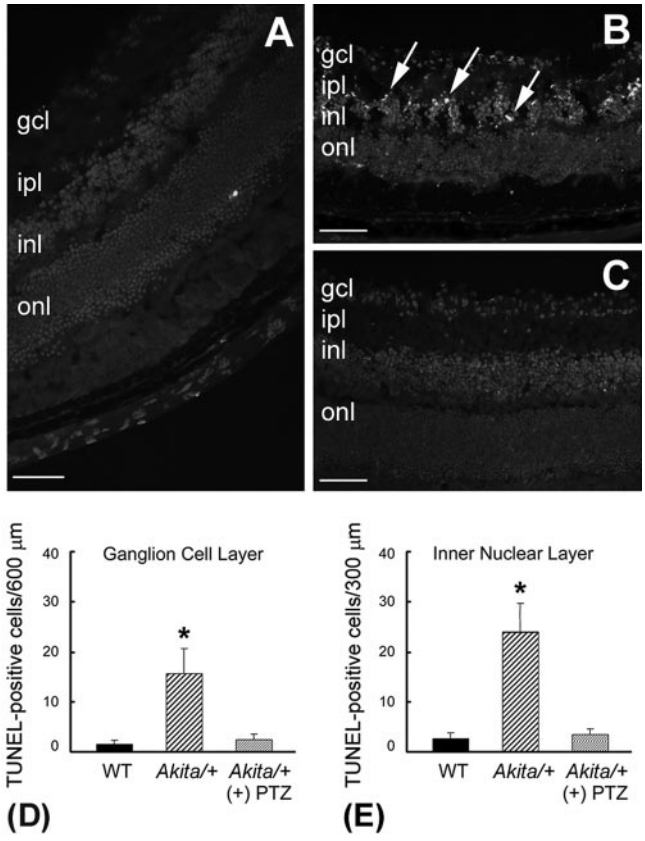

Figure 4. Neuronal apoptosis decreased in *Ins2*$^{Akita/+}$ mice administered (+)-pentazocine. TUNEL analysis of cryosections of retinas from (**A**) wild-type (25 weeks), (**B**) *Ins2*$^{Akita/+}$ (17–25 weeks after onset of diabetes), and (**C**) *Ins2*$^{Akita/+}$ (+)-pentazocine-treated mice (25 weeks). *Arrows*: numerous TUNEL^{+} cells in *Ins2*$^{Akita/+}$ mice (**B**). Quantitation of TUNEL^{+} cells in GCL (**D**) and INL (**E**). *Significantly different from wild-type and (+)-pentazocine-treated mice ($P < 0.001$).

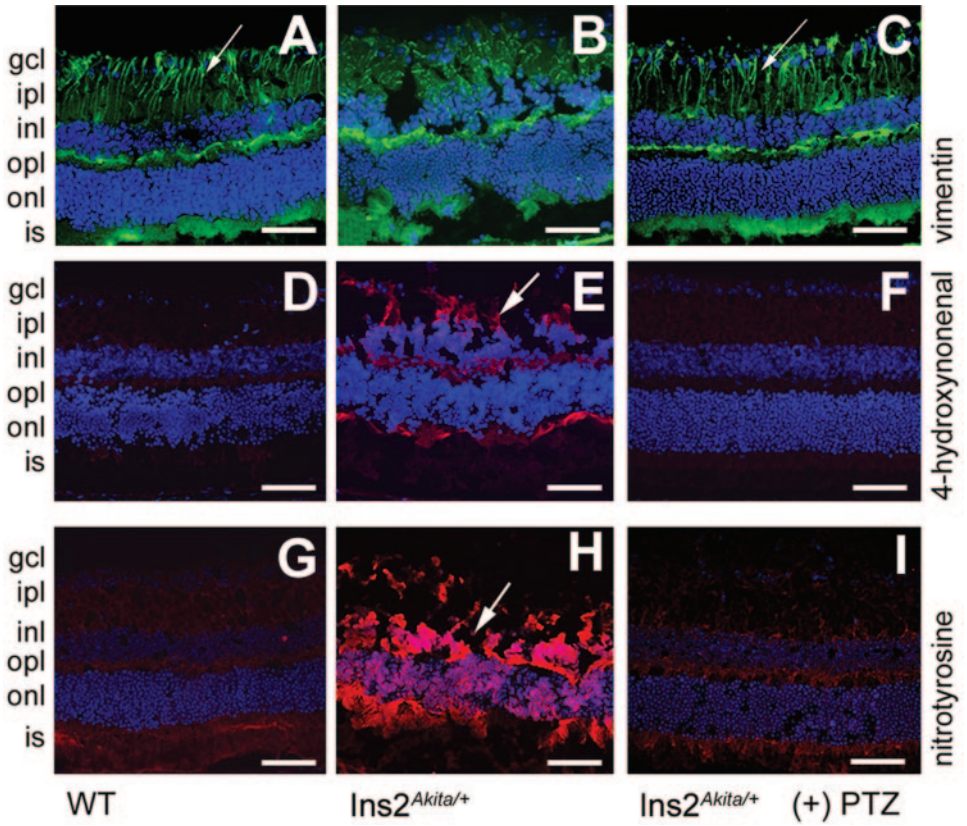

FIGURE 5. Oxidative stress was reduced in *Ins2*$^{Akita/+}$ mice administered (+)-pentazocine. (**A–C**) Immunodetection of vimentin labeling (*green* fluorescence) of radial glial fibers (*arrows*). Vimentin labeling of *Ins2*$^{Akita/+}$ retinas (**B**) was disrupted compared with that in wild-type (**A**) and (+)-pentazocine-treated *Ins2*$^{Akita/+}$ mice (**B**). (**D–I**) Immunodetection of 4-hydroxynonenal (**D–F**) and nitrotyrosine (**G–I**), oxidative stress and nitrative stress markers (*bright red* fluorescence, *arrows*), respectively, in *Ins2*$^{Akita/+}$ were increased compared with wild-type and (+)-pentazocine-treated *Ins2*$^{Akita/+}$ mice. PTZ, pentazocine; gcl, ganglion cell layer; ipl, inner plexiform layer; inl, inner nuclear layer; onl; outer nuclear layer, is; inner segments of photoreceptor cells. Scale bar, 50 μm.

Ins2$^{Akita/+}$ mouse retinas displayed disrupted, punctate labeling of fibers (Fig. 5B) whereas (+)-pentazocine-treated *Ins2*$^{Akita/+}$ mouse retinas had well-organized fibers comparable to wild-type retinas (Figs. 5A, 5C). Given the major role of Müller cells in maintaining retinal structural integrity, the disruption of fibers may contribute to the progressive damage observed in diabetic retinas; treatment of *Ins2*$^{Akita/+}$ mice with (+)-pentazocine preserved the radial organization. Reactive oxygen and nitrogen species have been implicated in the pathogenesis of diabetic retinopathy.[38–40] We analyzed the levels of 4-hydroxynonenal and protein-nitrotyrosine, markers of lipid peroxidation and reactive nitrogen species, respectively, in retinas of *Ins2*$^{Akita/+}$ mice compared with wild-type and (+)-pentazocine-treated *Ins2*$^{Akita/+}$ mice. There was increased immunodetection of these markers in *Ins2*$^{Akita/+}$ mice (Figs. 5E, 5H). Treatment with (+)-pentazocine (Figs. 5F, 5I) decreased the levels and were comparable to wild-type (Figs. 5D, 5G), suggesting that (+)-pentazocine reduces oxidative and nitrosative stress in diabetic retina.

The cell loss quantified in the present study (Fig. 3) is consistent with that reported for *Ins2*$^{Akita/+}$ mice by Barber et al.[33] In that study, the eyes were fixed in 4% paraformaldehyde and were subjected to cryosection/tape-transfer methodology. The morphology of the retinas of wild-type and pentazocine-treated *Ins2*$^{Akita/+}$ mice in the present study was well-preserved; however, cryoembedding, especially without fixation, can have untoward effects on retinal morphology, particularly if the retina is degenerating. Cryoembedding retinal tissue retains antigenicity and thus is advantageous for detection of markers of apoptosis and cellular stress (as needed for data presented in Figs. 4, 5); however, it does not preserve retinal architecture structure as well as other histologic processing methods. Hence retinas of nine additional mice were fixed in a formaldehyde-glutaraldehyde solution and processed for embedding in resin (Embed 812; Electron Microscopy Sciences). Figure 6 shows representative images from these specimens. The retinas of wild-type mice were well organized, with the ganglion cells being evenly distributed and the INL of a uniform thickness (~6–7 rows, Fig. 6A). Cells in both of these layers had lightly stained cytoplasm, and most had a plump, round shape. The retinas of the pentazocine-treated *Ins2*$^{Akita/+}$ mice had excellent morphology, an appearance similar to wild-type (Fig. 6D). The retinas of the *Ins2*$^{Akita/+}$ mice showed somewhat improved morphology than was observed with cryosec-

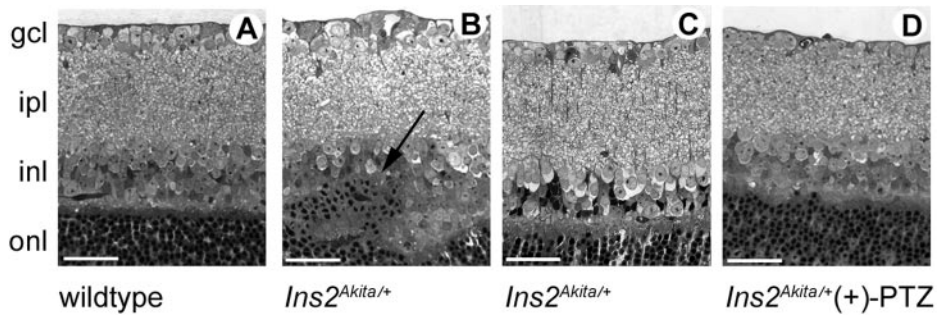

FIGURE 6. Eyes harvested from wild-type, *Ins2*$^{Akita/+}$ and (+)-pentazocine-treated *Ins2*$^{Akita/+}$ mice (age 12 weeks) fixed in paraformaldehyde/glutaraldehyde and embedded in resin. Representative retinas are shown from (**A**) wild-type, (**B**, **C**) *Ins2*$^{Akita/+}$, and (**D**) (+)-pentazocine-treated *Ins2*$^{Akita/+}$ mice. PTZ, pentazocine, gcl, ganglion cell layer, ipl, inner plexiform layer, inl, inner nuclear layer; onl, outer nuclear layer. Scale bar, 25 μm.

tioning (compare with Fig. 3); however, disruption in the INL–OPL interface continued to be evident (Fig. 6B, arrow). Cells of the GCL had a variable appearance. Some were plump and round adjacent to others that were shrunken and darkly stained, indicative of cells that are dying. The INL of the *Ins2*$^{Akita/+}$ mice had approximately four to five rows of cells. There were noticeable gaps between many of the cells that were not observed in the wild-type mice or in the *Ins2*$^{Akita/+}$ mice treated with (+)-pentazocine. These data of fixed retinal specimens are consistent with data obtained from the unfixed specimens and reflect cellular loss in the retinas of the *Ins2*$^{Akita/+}$ mice, which can be prevented by administration of (+)-pentazocine.

Discussion

This study represents the first report of the neuroprotective effects of the σR1 ligand (+)-pentazocine in an in vivo model of spontaneously arising retinopathy. The model we chose for our detailed analysis of the effects of (+)-pentazocine, the *Ins2*$^{Akita/+}$ mouse, was an ideal animal in which to test neuroprotection because of the quantifiable loss of retinal neurons over a relatively short time (4–5 months).[33] The observation that the σR1 gene and protein continued to be expressed in the mutant mice indicated that the appropriate target for the (+)-pentazocine treatment was available. (+)-Pentazocine is widely regarded as a potent and highly specific σR1 ligand based on pharmacologic studies.[41] It binds σR1 with a very high affinity and is presumed to be an agonist for the receptor; however, because the actual signaling events associated with σR1 activation have not been characterized, it is difficult to ascribe definitively an agonist or antagonist function to this ligand. It is for that reason that in the present study we did not test other compounds (i.e., presumed antagonists of σR1), to demonstrate specificity of the effect. The most convincing molecular evidence that (+)-pentazocine is specific for σR1 comes from analysis of the σR1 knockout mice (*mσR1*$^{-/-}$ mice) developed in the Montoliu laboratory.[42] Northern blot and Western blot analysis of multiple organs known to express σR1 (liver, kidney, brain, and heart) revealed no specific mRNAs for the mouse *σR1* gene or protein in any of these organs in the homozygous (knockout mice), whereas expression was reduced by half in heterozygous compared with wild-type mice. When brain membranes from the *mσR1*$^{-/-}$ mice were analyzed in binding assays with [^{3}H](+)pentazocine used as the radioligand, no binding activity in brain membranes was observed, and binding activity was reduced by half in heterozygous compared with wild-type animals (as shown in Fig. 3 of Ref. 42). Therefore, we conclude that the effects of (+)-pentazocine observed in the present study are due to effects on σR1.

The biweekly exposure of the *Ins2*$^{Akita/+}$ mice to (+)-pentazocine led to marked preservation of retinal structure. The morphology of the treated mice was excellent. The number of cells in the GCL in the (+)-pentazocine-treated *Ins2*$^{Akita/+}$ mice was comparable to the number in the wild-type. The inner nuclear and plexiform layers were of a thickness comparable to those in the wild-type.

Of interest, the preservation of retinal architecture and reduction of neuronal apoptosis did not appear to be a direct function of decreased hyperglycemia, because the (+)-pentazocine-injected *Ins2*$^{Akita/+}$ mice demonstrate marked elevation of blood glucose through the time of death. This finding is important and raises the question of whether retinal neuronal loss associated with diabetes involves hyperglycemia directly or whether it is due to complications secondary to hyperglycemia, such as oxidative stress. Our analysis of markers of cellular stress (4-hydroxynonenal, nitrotyrosine) showed a marked increase in expression in the *Ins2*$^{Akita/+}$ retinas, but a sharp quenching of these stress indicators in the presence of (+)-pentazocine. These findings are interesting in light of reports that ligands for σR1 can reduce NO production[13,43,44] and oxidative stress.[45] It is noteworthy that increased σR1 binding activity was observed in vitro when retinal Müller cells were treated with NO donors and donors of reactive oxygen species.[21]

The variable appearance of the mutant *Ins2*$^{Akita/+}$ retinas was intriguing and is reminiscent of the histologic features of retinas reported in studies of patients with diabetes[29,38] in which ganglion cell loss is extensive and INL disruption and cell loss are substantial. The alteration in retinal organization suggested that the scaffolding of the retina may be compromised. The cells known to be involved in such organization are the Müller cells and disruptions of Müller glial cells have been reported in diabetic retinopathy.[39,40] Our immunolabeling studies of vimentin, a Müller cell marker, showed punctate labeling in the *Ins2*$^{Akita/+}$ mouse retinas, but well-organized radial fibers in the (+)-pentazocine-treated animals. It would be interesting in future studies to isolate Müller cells from the *Ins2*$^{Akita/+}$and assess their myriad functions (e.g., transport activities), in the presence and absence of (+)-pentazocine.

In summary, we found that the σR1 ligand (+)-pentazocine afforded robust protection against retinal degeneration observed in *Ins2*$^{Akita/+}$ mice, a mouse model of spontaneously arising diabetes. The cell loss, neuronal apoptosis, marked disruption of retinal layers, and increased oxidative stress were prevented by treatment with (+)-pentazocine. The results are encouraging, because ligands for σR1 are already used clinically in the treatment of other diseases, including neuropsychiatric diseases (schizophrenia, depression, and cognitive disorders).[46] Promising results from the Bucolo laboratory in work involving acute injury-induced models in rat retina and new forms of σR1 ligands suggest that σR1 is a very attractive target for therapeutic intervention of retinal disease.[47] It remains to be determined whether other models of spontaneously arising nonacute retinal degeneration—for example, models of glaucoma—will respond positively to (+)-pentazocine. In addition, it is not known whether the treatment with (+)-pentazocine must start at the onset of disease, as performed in the present study, or whether delayed treatment would prove similarly beneficial. Currently, in vitro studies are under way to determine how (+)-pentazocine regulates genes involved in retinal neuronal apoptosis and will set the stage for elucidating the mechanism of in vivo neuroprotection observed in the present work.

Acknowledgments

The authors thank Guoliang Jiang, Leena Amarnath, Tracy K. Van Ells Moister, Weiguo Li, and Angeline Martin-Studdard for excellent technical assistance.

References

1. Hayashi T, Su TP. Sigma-1 receptor chaperones at the ER-mitochondrion interface regulate Ca (2+) signaling and cell survival. *Cell*. 2007;131:596–610.
2. Quirion R, Bowen WD, Itzhak Y, et al. A proposal for the classification of sigma binding sites. *Trends Pharmacol Sci*. 1992;13:85–86.
3. Hanner M, Moebius FF, Flandorfer A, et al. Purification, molecular cloning, and expression of the mammalian sigma 1-binding site. *Proc Natl Acad Sci USA*. 1996;93:8072–8077.
4. Kekuda R, Prasad PD, Fei YJ, Leibach FH, Ganapathy V. Cloning and functional expression of the human type 1 sigma receptor (hSigmaR1). *Biochem Biophys Res Commun*. 1996;229:553–558.
5. Prasad PD, Li HW, Fei YJ, et al. Exon-intron structure, analysis of promoter region, and chromosomal localization of the human type 1 sigma receptor gene. *J Neurochem*. 1998;70:443–451.

6. Seth P, Leibach FH, Ganapathy V. Cloning and structural analysis of the cDNA and the gene encoding the murine Type 1 sigma receptor. *Biochem Biophys Res Commun*. 1997;241:535–540.
7. Seth P, Fei YJ, Li HW, Huang W, Leibach FH, Ganapathy V. Cloning and functional characterization of a sigma receptor from rat brain. *J Neurochem*. 1998;70:922–931.
8. Dun Y, Thangaraju M, Prasad P, Ganapathy V, Smith SB. Prevention of excitotoxicity in primary retinal ganglion cells by (+)-pentazocine, a sigma receptor-1 specific ligand. *Invest Ophthalmol Vis Sci*. 2007;48:4785–4794.
9. Yang S, Bhardwaj A, Cheng J, Alkayed NJ, Hurn PD, Kirsch JR. Sigma receptor agonists provide neuroprotection in vitro by preserving bcl-2. *Anesth Analg*. 2007;104:1179–1184.
10. Meunier J, Ieni J, Maurice T. The anti-amnesic and neuroprotective effects of donepezil against amyloid beta25–35 peptide-induced toxicity in mice involve an interaction with the sigma1receptor. *Br J Pharmacol*. 2006;149:998–1012.
11. Katnik C, Guerrero WR, Pennypacker KR, Herrera Y, Cuevas J. Sigma-1 receptor activation prevents intracellular calcium dysregulation in cortical neurons during in vitro ischemia. *J Pharmacol Exp Ther*. 2006;319:1355–1365.
12. Maurice T, Grégoire C, Espallergues J. Neuro(active)steroids actions at the neuromodulatory sigma1 (sigma1) receptor: biochemical and physiological evidences, consequences in neuroprotection. *Pharmacol Biochem Behav*. 2006;84:581–597.
13. Vagnerova K, Hurn PD, Bhardwaj A, Kirsch JR. Sigma 1 receptor agonists act as neuroprotective drugs through inhibition of inducible nitric oxide synthase. *Anesth Analg*. 2006;103:430–434.
14. Meunier J, Ieni J, Maurice T. Antiamnesic and neuroprotective effects of donepezil against learning impairments induced in mice by exposure to carbon monoxide gas. *J Pharmacol Exp Ther*. 2006;317:1307–1319.
15. Schoenwald RD, Barfknecht CF, Xia E, Newton RE. The presence of sigma-receptors in the lacrimal gland. *J Ocul Pharmacol*. 1993; 9:125–139.
16. Bucolo C, Campana G, Di Toro R, Cacciaguerra S, Spampinato S. Sigma 1 recognition sites in rabbit iris-ciliary body: topical sigma 1-site agonists lower intraocular pressure. *J Pharmaco Exp Ther*. 1999;289:1362–1369.
17. Wang L, Duncan G. Silencing of sigma-1 receptor induces cell death in human lens cells. *Exp Cell Res*. 2006;312:1439–1446.
18. Ola MS, Moore PM, El-Sherbeny A, et al. Expression pattern of sigma receptor 1 mRNA and protein in mammalian retina. *Mol Brain Res*. 2001;95:86–95.
19. Senda T, Matsuno K, Mita S. The presence of sigma receptor subtypes in bovine retinal membranes. *Exp Eye Res*. 1997;64:857–860.
20. Ola MS, Martin PM, Maddox D, et al. Analysis of sigma receptor (σR1) expression in retinal ganglion cells cultured under hyperglycemic conditions and in diabetic mice. *Mol Brain Res*. 2002; 107:97–107.
21. Jiang G, Mysona B, Dun Y, et al. Expression, subcellular localization and regulation of sigma receptor in retinal Müller cells. *Invest Ophthalmol Vis Sci*. 2006;47:5576–5582.
22. Martin PM, Ola MS, Agarwal N, Ganapathy V, Smith SB. The Sigma Receptor ligand (+)-pentazocine prevents apoptotic retinal ganglion cell death induced in vitro by homocysteine and glutamate. *Mol Brain Res*. 2004;123:66–75.
23. Antonetti DA, Barber AJ, Bronson SK, et al. Diabetic retinopathy: seeing beyond glucose-induced microvascular disease. *Diabetes*. 2006;55:2401–2411.
24. Barber AJ. A new view of diabetic retinopathy: a neurodegenerative disease of the eye. *Prog Neuropsychopharmacol Biol Psychiatry*. 2003;27:283–290.
25. Roy MS, Gunkel RD, Podgor MJ. Color vision defects in early diabetic retinopathy. *Arch Ophthalmol*. 1986;104:225–228.
26. Hirsh J, Puklin J. Reduced contrast sensitivity may precede clinically observable retinopathy in type 1 diabetes. In: Henkind P, ed. *Acta XXIV International Congress of Ophthalmology.* New York: JB Lippincott; 1982:719–724.
27. Greco AV, Di Leo MA, Caputo S, et al. Early selective neuroretinal disorder in prepubertal type 1 (insulin-dependent) diabetic children without microvascular abnormalities. *Acta Diabetol*. 1994; 31:98–102.
28. Ghirlanda G, Di Leo MA, Caputo S, et al. Detection of inner retina dysfunction by steady-state focal electroretinogram pattern and flicker in early IDDM. *Diabetes*. 1991;40:1122–1127.
29. Abu-El-Asrar AM, Dralands L, Missotten L, Al-Jadaan IA, Geboes K. Expression of apoptosis markers in the retinas of human subjects with diabetes. *Invest Ophthalmol Vis Sci*. 2004;45:2760–2766.
30. Barber AJ, Lieth E, Khin SA, Antonetti DA, Buchanan AG, Gardner TW. Neural apoptosis in the retina during experimental and human diabetes: early onset and effect of insulin. *J Clin Invest*. 1998;102:783–791.
31. Bek T. Transretinal histopathological changes in capillary-free areas of diabetic retinopathy. *Acta Ophthalmol* (*Copenh*). 1994;72: 409–415.
32. Kerrigan LA, Zack DJ, Quigley HA, Smith SD, Pease ME. TUNEL-positive ganglion cells in human primary open-angle glaucoma. *Arch Ophthalmol*. 1997;115:1031–1035.
33. Barber AJ, Antonetti DA, Kern TS, et al. The *Ins2*^{Akita} mouse as a model of early retinal complications in diabetes. *Invest Ophthalmol Vis Sci*. 2005;46:2210–2218.
34. Martin PM, Roon P, Van Ells TK, Ganapathy V, Smith SB. Death of retinal neurons in streptozotocin-induced diabetic mice. *Invest Ophthalmol Vis Sci*. 2004;45:3330–3336.
35. Yoshioka M, Kayo T, Ikeda T, Koizumi A. A novel locus, Mody4, distal to D7Mit189 on chromosome 7 determines early-onset NIDDM in nonobese C57BL/6 (Akita) mutant mice. *Diabetes*. 1997;46:887–894.
36. Dun Y, Mysona B, Van Ells TK, et al. Expression of the glutamate-cysteine (x_c^-) exchanger in cultured retinal ganglion cells and regulation by nitric oxide and oxidative stress. *Cell Tissue Res*. 2006;324:189–202.
37. Moore P, El-Sherbeny A, Roon P, Schoenlein PV, Ganapathy V, Smith SB. Apoptotic retinal ganglion cell death is induced in vivo by the excitatory amino acid homocysteine. *Exp Eye Res*. 2001; 73:45–57.
38. Abu El-Asrar AM, Meersschaert A, Dralands L, Missotten L, Geboes K. Inducible nitric oxide synthase and vascular endothelial growth factor are colocalized in the retinas of human subjects with diabetes. *Eye*. 2004;18:306–313.
39. Du Y, Sarthy VP, Kern TS. Interaction between NO and COX pathways in retinal cells exposed to elevated glucose and retina of diabetic rats. *Am J Physiol Regul Integr Comp Physiol*. 2004;287: R735–R741.
40. Zhan X, Du Y, Crabb JS, Gu X, Kern TS, Crabb JW. Targets of tyrosine nitration in diabetic rat retina. *Mol Cell Proteomics*. 2008; 7(5):864–874.
41. de Costa BR, Bowen WD, Hellewell SB, et al. Synthesis and evaluation of optically pure [3H]-(+)-pentazocine, a highly potent and selective radioligand for sigma receptors. *FEBS Lett*. 1989;251:53–58.
42. Langa F, Codony X, Tovar V, et al. Generation and phenotypic analysis of sigma receptor type I (sigma 1) knockout mice. *Eur J Neurosci*. 2003;18:2188–2196.
43. Bhardwaj A, Sawada M, London ED, Koehler RC, Traystman RJ, Kirsch JR. Potent sigma1-receptor ligand 4-phenyl-1-(4-phenylbutyl) piperidine modulates basal and N-methyl-D-aspartate–evoked nitric oxide production in vivo. *Stroke*. 1998;29:2404–2411.
44. Goyagi T, Goto S, Bhardwaj A, Dawson VL, Hurn PD, Kirsch JR. Neuroprotective effect of sigma(1)-receptor ligand 4-phenyl-1-(4-phenylbutyl) piperidine (PPBP) is linked to reduced neuronal nitric oxide production. *Stroke*. 2001;32:1613–1620.
45. Bucolo C, Drago F, Lin LR, Reddy VN. Sigma receptor ligands protect human retinal cells against oxidative stress. *Neuroreport*. 2006;17:287–291.
46. Hashimoto K, Ishiwata K. Sigma receptor ligands: possible application as therapeutic drugs and as radiopharmaceuticals. *Curr Pharm Des*. 2006;12:3857–3876.
47. Cantarella G, Bucolo C, Di Benedetto G, et al. Protective effects of the sigma agonist Pre-084 in the rat retina. *Br J Ophthalmol*. 2007;91:1382–1384.